

Empirical Modeling of Sea-Level Pressure Variability

S. Kravtsov^{1,2}, N. Tilinina², Y. Zyulyaeva² and S. Gulev²

¹University of Wisconsin-Milwaukee, Department of Mathematical Sciences, Atmospheric Sciences Group

² P. P. Shirshov Institute of Oceanology, Moscow, Russia

Motivation and methods

We have developed an empirical stochastic model capable of emulating and predicting evolution of the sea-level pressure (SLP). The model was trained on the 6-hourly, 0.75° resolution Northern Hemisphere's SLP data from the 1979–2013 ERA-Interim Reanalysis (Dee et al. 2011).

The process of model construction involves several steps. First, we subtract from the full data the monthly SLP climatology and form daily-mean SLPA anomalies. Next, the resulting daily SLPA anomalies are projected onto its 1000 leading Empirical Orthogonal Functions (EOFs: Monahan et al. 2009), which account for over 99% of the total SLPA variability. The stochastic ARMA model for the SLPA principal components \mathbf{x} is postulated to have the following multi-level form (Kravtsov et al. 2005) [$d\mathbf{x} = \mathbf{x}^{n+1} - \mathbf{x}^n$]:

$$d\mathbf{x} = \mathbf{x} \cdot \mathbf{A}^{(1)} + \mathbf{r}^{(1)},$$

$$d\mathbf{r}^{(1)} = [\mathbf{r}^{(1)} \mathbf{x}] \cdot \mathbf{A}^{(2)} + \mathbf{r}^{(2)}, \quad (1)$$

$$d\mathbf{r}^{(2)} = [\mathbf{r}^{(2)} \mathbf{r}^{(1)} \mathbf{x}] \cdot \mathbf{A}^{(3)} + \mathbf{r}^{(3)},$$

the model's parameters are found via regularized multiple linear regression and depend on seasonal cycle at monthly resolution.

At the stage of model simulation, the residual forcing at the third model level $\mathbf{r}^{(3)}$ is chosen via random sampling from the library of the observed residuals in a way conditioned on the simulated state \mathbf{x} . The simulated daily anomalies are also used to model, empirically, the 6-hourly SLPA residuals. The resulting 6-hourly SLPA anomalies are transformed back to physical space and, after adding the mean seasonal cycle, represent an emulation of the full SLP time series.

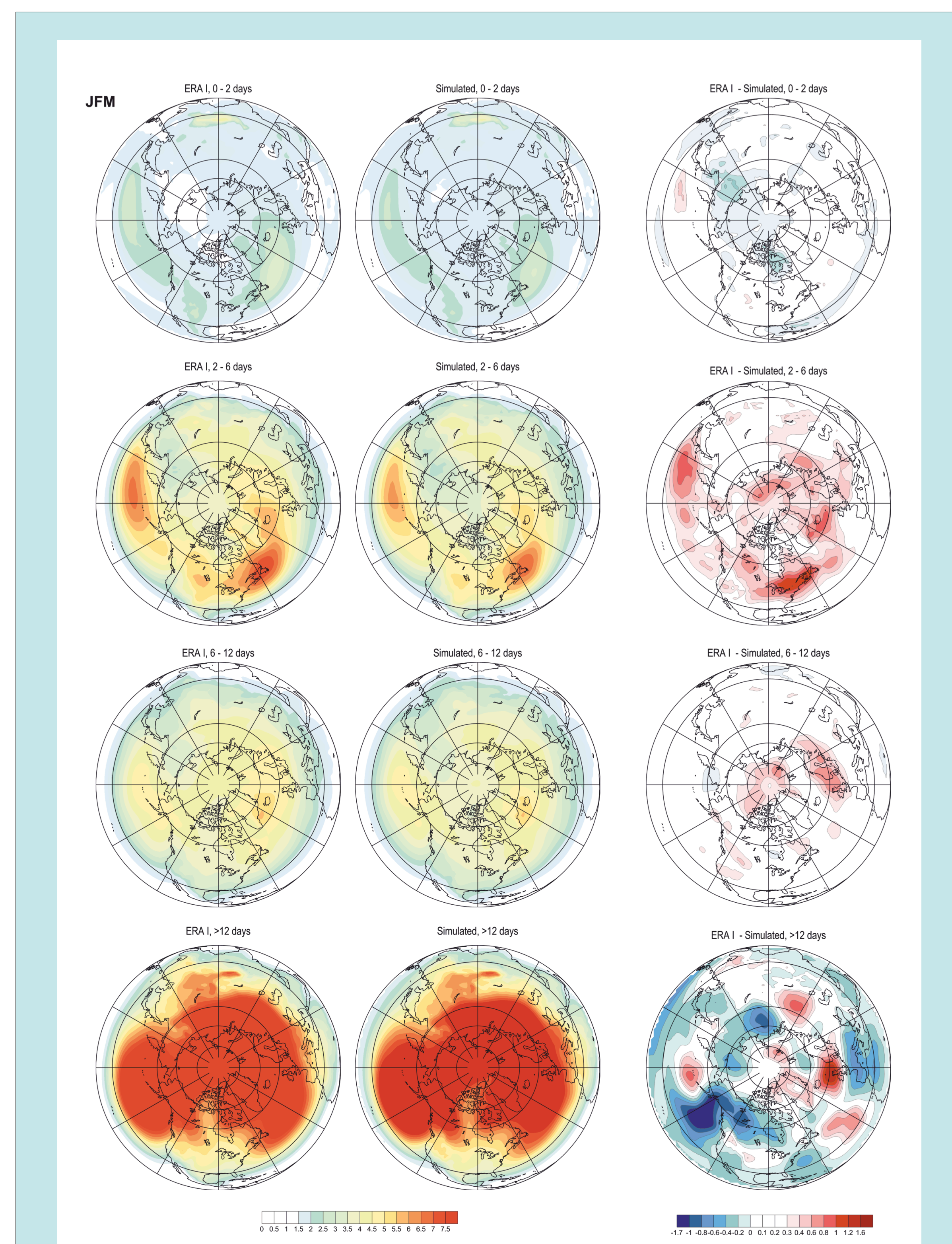


Figure 1: Standard deviations (hPa) of the wintertime (JFM) observed (left column) and simulated (middle column) band-pass filtered SLPA anomalies in physical space; the difference (observed – simulated) is shown in the right column. The four rows (top to bottom) correspond to the 2-day high-pass filtered, 2–6-day and 6–12-day band-pass filtered, and 12-day low-pass filtered anomalies, respectively.

Model performance

The model captures well both the observed magnitude and patterns, as well as the seasonal cycle of the **band-pass filtered variance** (Fig. 1). In Fig. 1, the only statistically significant difference between the observed and simulated variance appears is the most pronounced negative difference seen over the Pacific Ocean.

Another essential aspect of the observed variability one would want the empirical model simulation to reproduce concerns **the propagation of SLPA anomalies**. One way to diagnose such propagation is to construct one-point lagged correlation maps (see Fig. 2). In this particular case — for the year and the location chosen to be in the middle of Pacific Ocean, — there turned out to be a near-perfect correspondence in the pattern and speed of the observed and simulated SLPA propagation in both the 0–2-day and 2–6-day spectral bands (note that we don't expect to match the exact history of the simulated “1980” to that of the observed 1980 — and only attempt to reproduce the overall statistics of the SLP variability).

Similar impressive match is documented between **the spatial density of the observed and simulated cyclones** tracked using the algorithm of Rudeva and Gulev (2007); the model, however, slightly underestimates the number of cyclones relative to observations (Fig. 3).

Finally, the simulated cyclones' life cycles exhibit spatiotemporal characteristics that closely resemble those of the observed cyclones. As an example, **Figure 2** shows two-dimensional histograms of the cyclone propagation speeds/deepening rates for observations and model simulation.

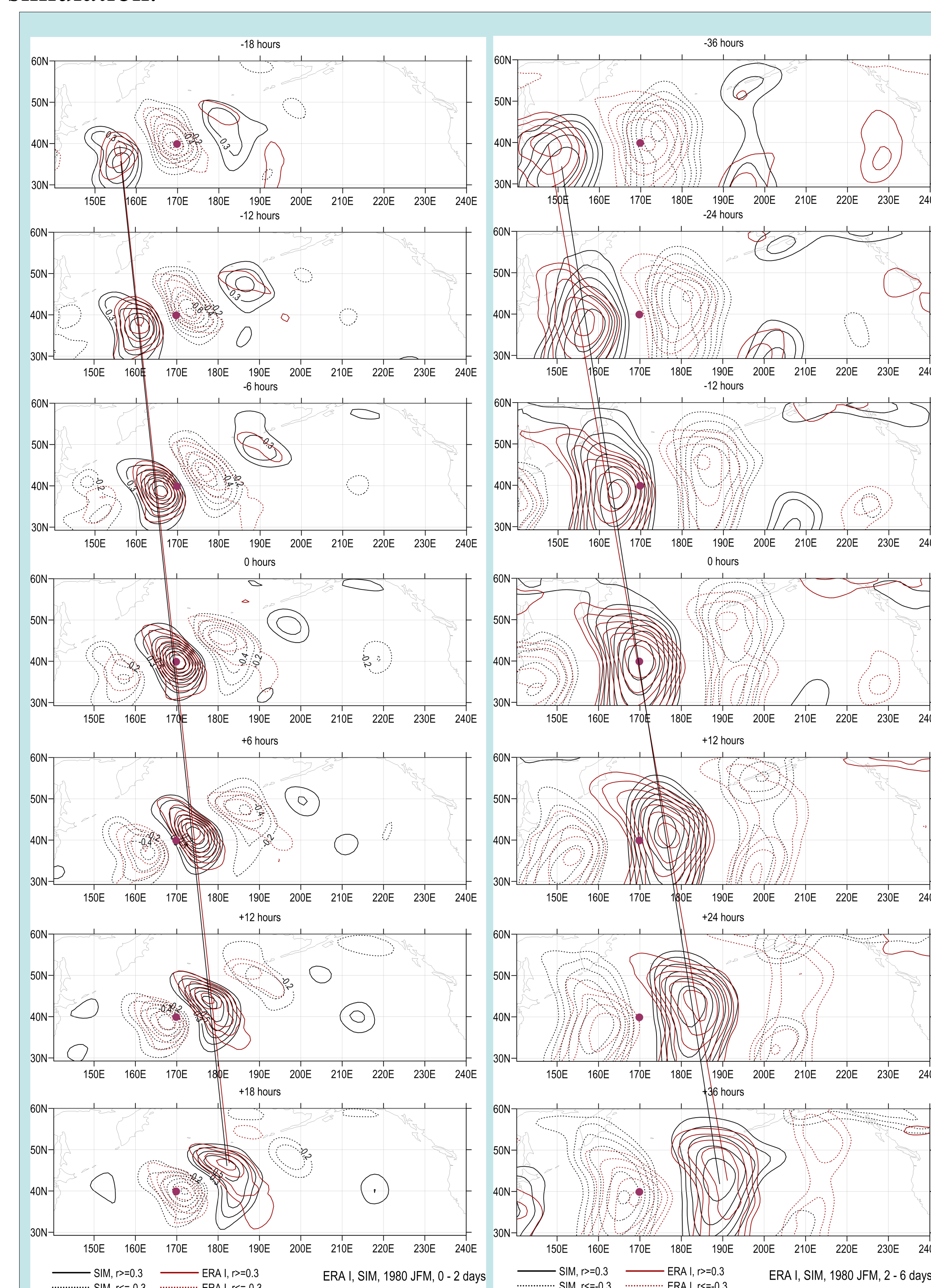


Figure 2: SLP anomaly propagation in observations and stochastic simulation. Shown are one-point lagged correlation maps for the observed (red contours) and simulated (black contours) wintertime (JFM) data for the year 1980 relative to the point 40°N, 170°E in the Pacific region. The values of lags are given in the caption of each panel. Left column: propagation of the 2-day high-pass filtered anomalies; right column: propagation of the 2–6-day band-pass filtered anomalies.

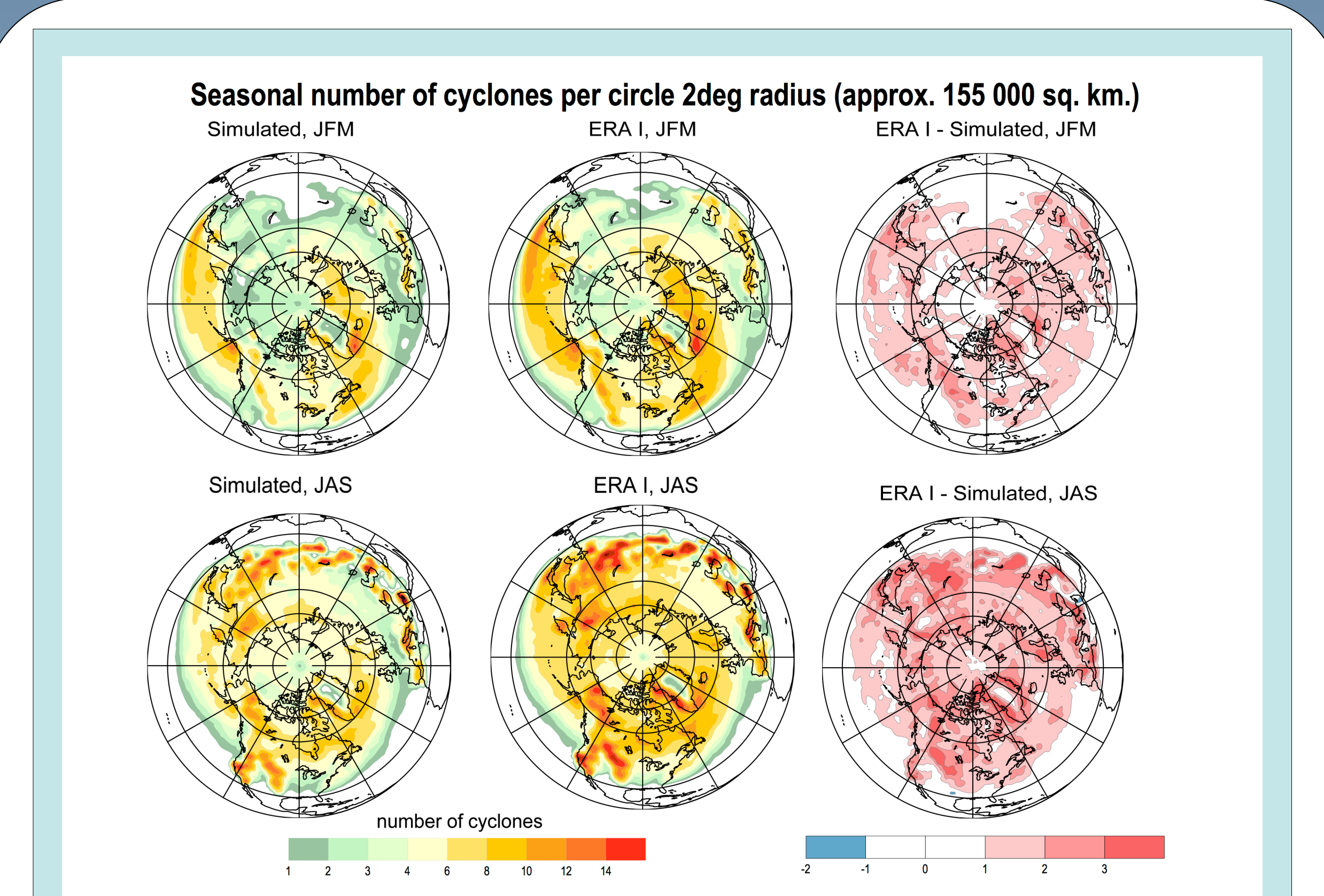


Figure 3: Spatial density of cyclones in the observed (left column) and simulated (middle column) data the difference (simulated – observed) is given in the right column. Top row: winter season (JFM); bottom row: summer season (JAS).

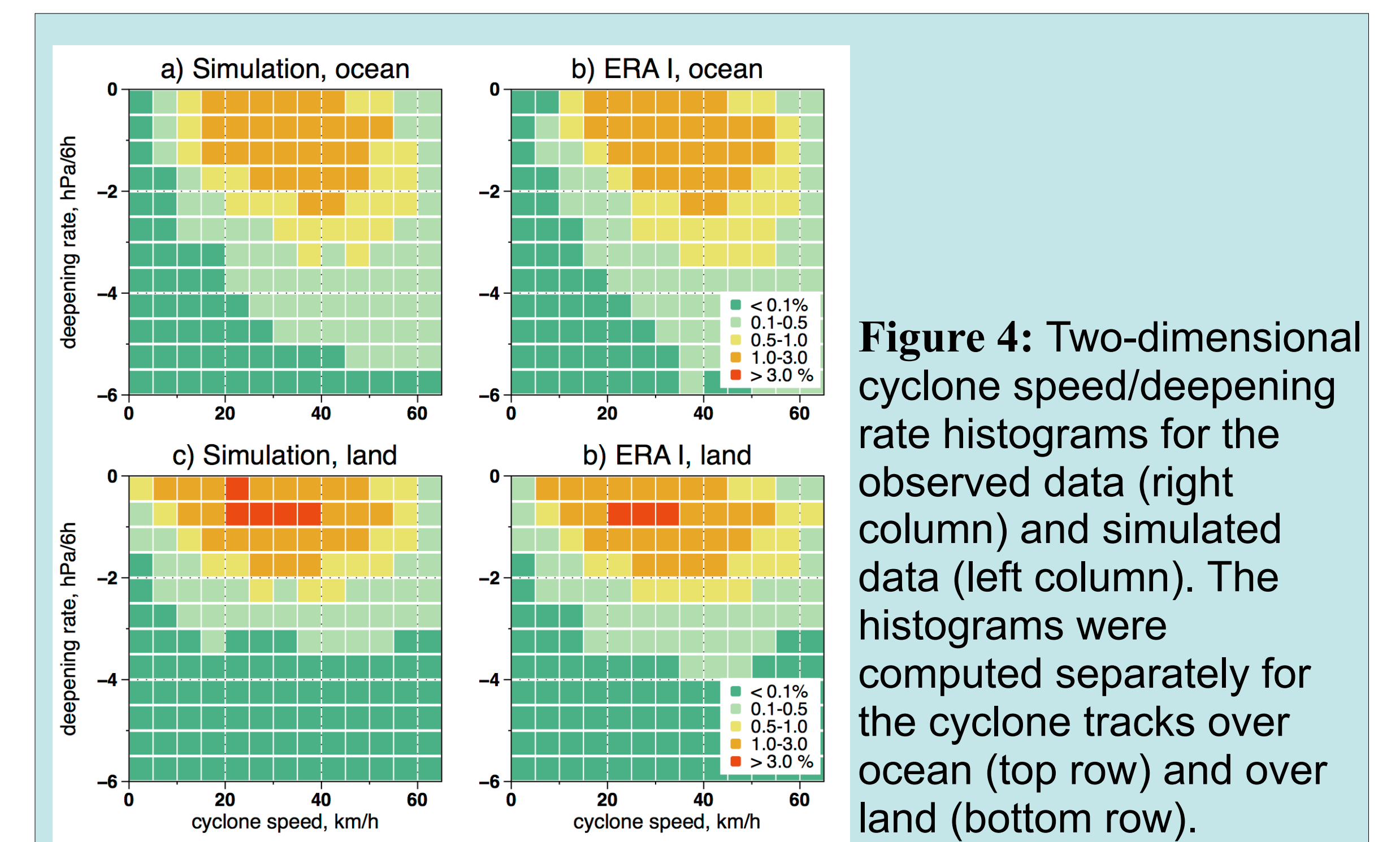


Figure 4: Two-dimensional cyclone speed/deepening rate histograms for the observed data (right column) and simulated data (left column). The histograms were computed separately for the cyclone tracks over ocean (top row) and over land (bottom row).

Discussion

The Earth's climate involves dynamical interactions across a wide range of spatial and time scales. Given a relatively short duration of the observed instrumental records, the climatic data modeling thus far concentrated on reproducing relatively low-dimensional subsets of the observed climate evolution (Penland 1989, 1996). A daring — and to a large extent successful — attempt of this study was to try to describe, statistically, as much as possible of the observed variability in a select but important climatic field, namely the SLP. Our ability to construct such a skillful empirical SLP model demonstrates that the number of effective (spatial) degrees of freedom in the observed climate variability is not that large and that the observed data record is not that short for the comprehensive statistical data modeling to be infeasible. The model constructed in this paper is also a proof-of-concept, prototype model and, as such, provides the methodology for simulating other climatic fields.

Bibliography

- Dee, et al., 2011. *Quart. J. Roy. Meteor. Soc.*, **137**, 553–597.
 Kravtsov, S., et al., 2005. *J. Climate*, **18**, 4404–4424.
 Monahan, A., et al., 2009. *J. Climate*, **22**, 6501–6514.
 Penland, C., 1989. *Mon. Wea. Rev.*, **117**, 2165–2185.
 Penland, C., 1996. *Physica D*, **98**, 534–558.
 Rudeva and Gulev, 2007. *Mon. Wea. Rev.*, **135**, 2568–2587.

Acknowledgement. This work was funded by the NSF grants OCE-1243158 and AGS-1408897 (SK) and the contract with Russian Ministry of Education and Science 14.B25.31.0026 (NT, YZ, SKG).
For further information please contact kravtsov@uwm.edu. PDF version: https://pantherfile.uwm.edu/kravtsov/www/downloads/AGU_Fall_2014_Kravtsov.PDF